ev. Mexicana Astron. Astrof., **21**, 633-637 (1990)

HARD X-RAY ARCMIN IMAGING WITH THE EXITE TELESCOPE

João Braga
Instituto de Pesquisas Espaciais

Corbin E. Covault, Raj Manandhar
and Jonathan E. Grindlay
Harvard-Smithsonian Center for Astrophysics

RESUMO: Neste trabalho descreve-se o "Energetic X-ray Imaging Telescope Experiment" (EXITE) e mostram-se os primeiros resultados obtidos. Discute-se o método de abertura codificada, utilizado em EXITE, para obtenção de imagens de fontes cósmicas de raios-X.

ABSTRACT: In this paper we describe the Energetic X-ray Imaging Telescope Experiment (EXITE) and show the first results obtained. We discuss the coded-aperture technique for imaging of cosmic X-ray sources, used by EXITE.

Key words: **INSTRUMENTS – X-RAYS – SOURCES**

INTRODUCTION

The Energetic X-ray Imaging Telescope Experiment (EXITE) is a balloon-borne imaging telescope for ectromagnetic radiation in the hard X-ray range. (Grindlay *et al.* 1986; Garcia *et al.* 1986). The high angular solution of EXITE can resolve the hard X-ray sources in the most crowded regions of the sky, like the Galactic Center, ıd is the best achieved by present instruments. The imaging capability is provided by the use of a coded-mask and a ›sition-sensitive X-ray detector. Recent improvements on the detector and gondola systems are reported by Covault, ːaga, and Grindlay (1988), and both calibration results and flight performance of EXITE are reported by Braga, ›vault and, Grindlay (1989). EXITE observed a variety of both galactic (Covault, Braga, and Grindlay, 1988*b* and ːtragalactic (Braga, Covault, and Grindlay, 1988) objects. In this paper we present preliminary results from EXITE ılloon flights, with emphasis on hard X-ray imaging of the Crab nebula, and discuss the coded-aperture technique r hard X-ray imaging of cosmic sources.

. INSTRUMENT DESCRIPTION

EXITE's central detector is a 6 mm-thick NaI(Tl) scintillator with total area of 934 cm^2, which is optically ıupled to a two-stage Thomson-CSF image intensifier tube (Rougeot, Roziere, and Driard, 1979). The system operates the energy range ~20 – 300 keV.

The first stage of the image intensifier has a light gain of ~ 30 and reduces the linear scale of the image ' a fractor of 16. The second stage of the tube is optically coupled to the first through a fiber optics plug, and contains silicon PIN diode which is used as a resistive anode readout. Electrons from the second stage photocathode are celerated into the position sensitive silicon PIN diode by a 15 kV potential, which causes the creation of ~ 4×10^3 ıarges per electron in the PIN diode. The overall gain is such that a 122 keV X-ray generates ~ 3×10^7 electron–hole ıirs in the PIN diode.

The electrons and holes generated in the intrinsic region diffuse to the P and N surfaces of the diode, ıd then diffuse through the resistive surface sheets to the four readout strips located at the edges of the diode. The ›o top strips are perpendicular to the two botton ones. Referring to the signal on the two top strips as x_1 and x_2, ıd on the botton y_1 and y_2, the X and Y positions of the incoming X-rays are given by $X = (x_1 - x_2)/(x_1 + x_2)$ and $= (y_1 - y_2)/(y_1 + y_2)$. The energy of the incident X-ray is proportional to $y_1 + y_2$ (which is the same as $x_1 + x_2$).

The spatial and energy resolution are dominated by the fluctuations in the number of photoelectrons emitted at the first stage photocathode. We measured an energy resolution of ~11 % for the 122 keV line of Co^{57} in the laboratory, whereas the spatial resolution for the same energy was determined to be ~6 mm FWHM. This energy resolution is ~50% better than previous experiments using scintillators. The spatial resolution, when combined with the distance of 2 meters between the detector and the coded mask, and a mask cell size of 13 mm, yield an angular resolution in the sky of ~32 arcmin FWHM at 100 keV. This resolution is not achieved by any experiment in operation currently what makes EXITE a very competitive imaging instrument for hard X-ray and low-energy γ-ray astronomy. Two 1-D crossed collimators, placed between the detector and the coded-mask, define the field of view to be 3.4° FWHM. The coded-mask is based on 13 mm-side square elements, made of 3 mm Pb, 2 mm Sn, and 1 mm Cu, and is "sandwhiched" between two layers of lexan for mechanical support. The basic pattern of the mask is a 11 × 13 "Uniformly Redundant Array" (Fenimore and Cannon 1978), which allows "perfect" imaging reconstruction (no intrinsic noise) with high sensitivity (large open area).

The EXITE detector system is surrounded by a graded passive shield (2 mm Pb, 1 mm Sn, and 1 mm Cu) which is wrapped around and behind the Thomson tube and extends forward to the collimator. This shield prevents photons with energies up to 300 keV from hitting the main NaI(Tl) detector. Surrounding the passive shielding there is a 4π steradians active shielding of plastic scintillator NE-102 for charged particle rejection, working in anti-coincidence with the NaI(Tl) detector.

The entire detector assembly is enclosed in a pressure vessel via a shock isolation system, designed to dampen the impulsive acceleration at parachute opening and landing impact to be ≤ 2 g which can be sustained by the image intensifier. The pressure vessel keeps the detector system at constant atmospheric pressure and temperature and is mounted to the elevation drive axis of the balloon gondola.

A balloon gondola design has been developed to allow the EXITE detector system to be flown and pointed with ~1 arcminute stability in a alt-az telescope configuration.

III. CODED-APERTURE TECHNIQUE

EXITE images are produced using the coded-aperture concept (Fenimore and Cannon 1978). The images are built via a cross-correlation process between the pattern of the coded-mask and the distribution of photons in the surface of the detector. In a digital analysis, we define the mask pattern as a matrix G where the openings of the mask are represented by "1" and the opaque elements by "−1". The distribution of photons (matrix P) is defined as the number of photons (for a given integration time) that hit an area on the detector surface equal to the mask cell area. Using these definitions, the reconstructed object $\hat{O}$ is given by:

$$\hat{O}(i,j) = \sum_k \sum_l P(k,l)G(k+i,l+j)$$

where $\hat{O}(i,j)$ is the number of photons, for a given integration time, coming from a "sky-bin" (which has an angular size defined by the mask cell size divided by the mask–detector distance) within the field-of-view of the telescope. The signal-to-noise ratio of an image constructed in such a way is given by:

$$SNR = \frac{N^{1/2} S_{ij}}{(S_{ij} + I_t + 2B)^{1/2}} \times f(E)$$

where N is the number of holes in the mask pattern, S_{ij} is the number of photons coming from a particular source, I_t is the contribution from all the other sources in the field-of-view, and B is the total number of background photons, all relative to one mask-cell area. $f(E)$ is an empirical factor that depends on the degree of smearing of the raw image which in turn is a function of the energy. For a perfectly sharp image, $f(E)$ would be 1, whereas for a very smeared shadow pattern, corresponding to a very poor spatial resolution on the detector, $f(E)$ would approach 0.

We have carried out a computer simulation to illustrate how the method works. In Figure 1 we show the photon distribution corresponding to 4,000 photons being detected by a position-sensitive detector with spatial resolution of the order of the mask cell size. 2 000 of these photons are coming from a source placed at infinity, at a angle of 1° with respect to the perpendicular to the detector surface. 1 000 photons are coming from another source placed 180° away in azimuth with respect to the first, and the other 1 000 photons are background counts. We can see that this distribution bears very little resemblance with the pattern of openings in the mask, but nevertheless the source original distribution in the field-of-view can be very clearly reconstructed, as it is shown in Figure 2. In the next section we will show an image of the Crab region obtained by EXITE using the method described above.

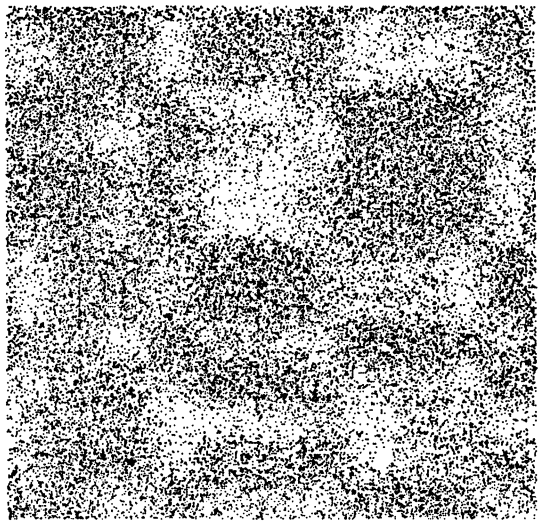

Fig.1. Simulated distribution of photons

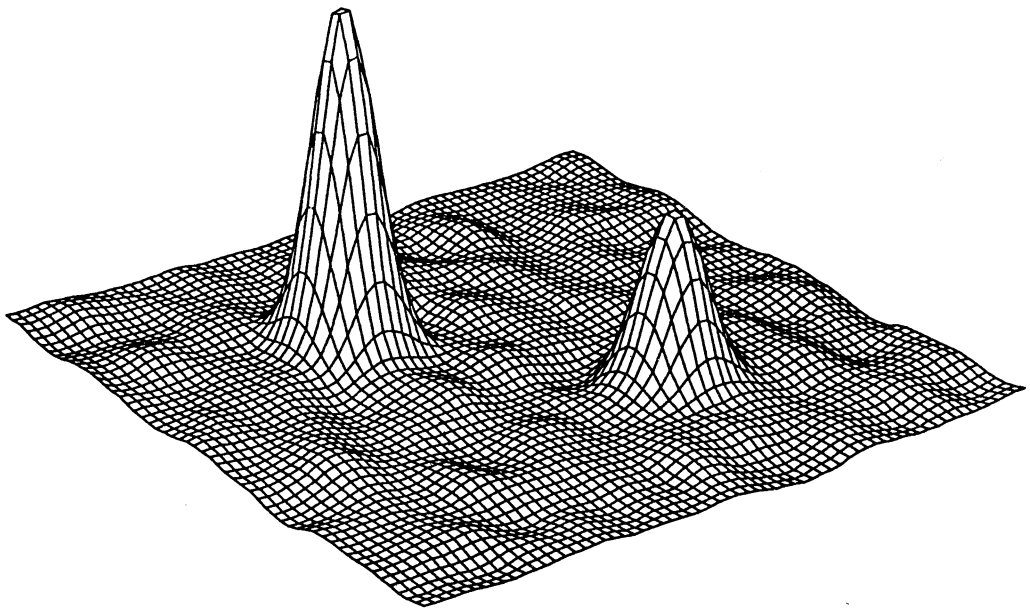

Fig. 2. Reconstructed image

IV. FIRST RESULTS—THE CRAB NEBULA

EXITE has been flown three times on board stratospheric balloons. The first flight was carried out in Alice Springs, Australia, on May 18, 1988, as part of the NASA campaign to observe the supernova 1987A. The launch occurred at 15:50 UT and the payload remained at float altitudes ($4g/cm^2$) for approximately 6 hours. Due to a totally unanticipated thermal-induced mechanical problem in which a portion of the telescope insulation slipped and prevented pointing of the telescope, the flight did not achieve its scientific objectives. Nevertheless, valuable engineering data on the detector and gondola performance were obtained. In particular, the efficiency of the detector shield system, both passive and active, was measured. Whereas on the ground the plastic anti-coincidence charged particle shield rejects only about 15 % of the total background in the 15-300 keV range of the detector, at float altitude a shield rejection of about 70 % was measured. The total background rate was ~225 counts/sec, which is comparable to the rate predicted from Monte Carlo simulations (Garcia *et al.* 1986).

The second balloon flight took place in Fort Sumner, NM. For this second flight, some modifications were made on both detector and gondola systems, which included: new foam insulation on the telescope, an RC network in the detector electronics for filtering against giant pulse events, new temperature sensors, and new delay lines and power supplies. EXITE was successfully launched on a 28 m.cu.ft. balloon at 23:40 UT October 8, 1988, and remained at float altitude for 19 hours. Several x-ray sources were observed, including the X-ray pulsar Her X-1, the X-ray binaries with black-hole candidates Cyg X-1 and A0620-00, the millisecond pulsar PSR1957+20, and the active galactic nuclei 3C 273, NGC 4151 and 0241+61. We have also looked at the Crab nebula for calibration purposes. The science data are currently being analysed and will be reported elsewhere. The background rate measured was ~350 counts/sec, which is about a factor of 1.5 higher than that measured in Australia. This is expected given the difference in geomagnetic latitude, and a similar factor has been obtained by many balloon experiments.The energy spectra of an on-board Cd^{109} radioactive source, taken every hour during the flight, showed a maximum energy gain variation of about 2 % throughout the flight.

The third balloon flight of EXITE took place again in Australia, as part of the last NASA campaign to observe the supernova 1987A. EXITE was launched from Alice Springs on May 8, 1989, 21:51 UT. The experiment remained at float altitude for ~ 29 hours at a residual atmosphere of ~ $3.5 g/cm^2$. All systems worked well in this flight and the data are currently being analysed. Besides the supernova, we observed other sources like the galactic center region, the transient source A0535+26, the X-ray pulsars Vela X-1 and GX 301-2, the black hole candidate GX 339-4, and the AGN MR 2251-17.

In Figure 3 we show an image of the Crab nebula obtained by EXITE in its second flight in Fort Sumner. This image has a significance of 10 σ for an integration time of 20 minutes. Due to flat-fielding problems, we only used about one third of the total detector area. The image showed is a 4°50'×4°08' square region, with a source location accuracy ~5 arcmin.

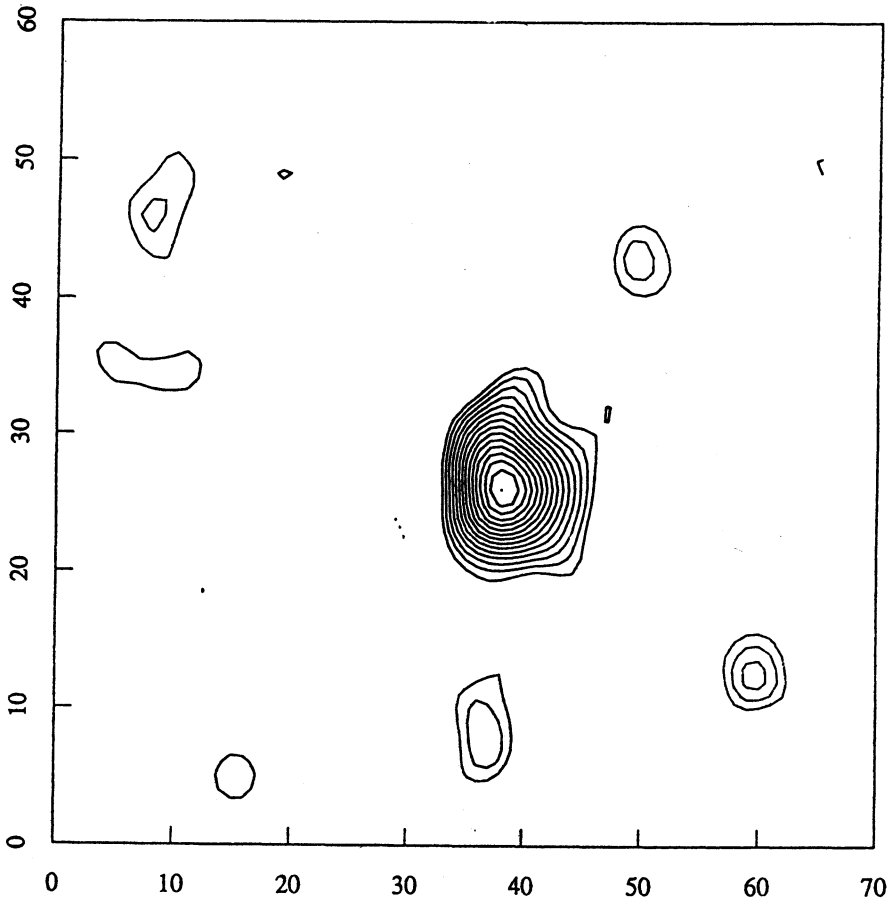

Fig. 3. EXITE image of the Crab nebula

We thank J. Gomes, G. Nystrom, V. Kuosmanen, F. Licata, J. D'Angelo and R. Scovel for technical support. J. Braga is deeply grateful to Prof. Jonathan E. Grindlay for the hospitality during his stay at the Harvard-Smithsonian Center for Astrophysics. J. Braga also gratefully acknowledges the Smithsonian Pre-doctoral Fellowship program and CNPq (Brazil) for support. C. Covault gratefully acknowledges the support of the NASA Graduate Student Researchers Program. This work is partially supported by NASA grant NAGW-624.

REFERENCES

Braga, J., Covault, C.E., and Grindlay, J.E. 1988, *Bull. of the A.A.S.*, **20**, 1024.

Braga, J., Covault, C.E., and Grindlay, J.E. 1989, *IEEE Transactions in Nuclear Science*, **36**, 871.

Covault, C.E., Braga, J., and Grindlay, J.E. 1988*a* in *Nuclear Spectroscopy of Astrophysical Sources*, ed. N. Gehrels and G.H. Share, AIP Conference Proceedings, **170**, 444.

Covault, C.E., Braga, J., and Grindlay, J.E. 1988*b* *Bull. A.A.S.*, **20**, 1056.

Fenimore, E.E. and Cannon, T.M. 1978, *Applied Optics*, **17**, 337.

Garcia, M.R., Grindlay, J.E., Burg, R.I., Murray, S.S., and Flanagan, J. 1986, *IEEE Transactions in Nuclear Science*, **33**, 735.

Grindlay, J.E., Garcia, M.R., Burg, R.I., and Murray, S.S. 1986, *IEEE Transactions in Nuclear Science* **33**, 750.

Rougeot, H., Roziere, G., Driard, B. 1979, in *Advances in Electronics and Electron Physics*, Academic Press, vol. **52**, 227.

João Braga: Departamento de Astrofísica, Instituto de Pesquisas Espaciais, C.P. 515, São José dos Campos, SP, CEP 12201, Brasil.

C. Covault, J. Grindlay and R. Manandhar: Center for Astrophysics, 60 Garden St, Cambridge, MA 02138, USA.